Journal of Nano- and Electronic Physics
Vol. **18** No 2, 02022(4pp) (2026)

Журнал нано- та електронної фізики
Том **18** № 2, 02022(4cc) (2026)

OPEN ACCESS

REGULAR ARTICLE

Performance Analysis of a *n*-i-*p* and *p*-i-*n* Structured Lead-Free Cs_2TiI_6 -Based Perovskite Solar Cell

K. Chakraborty[1,*], R. Narmadha[2,†], Islom Kadirov[3], Visalakshi Naraparedddi[4], Ranjan Kumar Mahapatra[5], Karedla Chitambara Rao[6]

[1] *Department of Electrical Engineering, IMPS College of Engineering and Technology, Malda, W.B, India*
[2] *Department of Mechatronics, Sathyabama Institute of Science and Technology, Chennai, T.N, India*
[3] *Department of Transport Systems, Urgench State University, Urgench, Uzbekistan*
[4] *School of Business, Aditya University, Surampalem, A.P, India*
[5] *Department of Electronics and Communication Engineering, Koneru Lakshmaiah Education Foundation, Guntur, A.P, India*
[6] *Department of Electronics and Communication Engineering, Aditya Institute of Technology and Management, Tekkali, A.P., India*

(Received 25 January 2026; revised manuscript received 19 April 2026; published online 29 April 2026)

This research work shows the development of an n-i-p structured FTO/TiO_2/Cs_2TiI_6/Spiro-OMeTAD/Au and a *p*-i-*n* structured FTO/PEDOT:PSS/Cs_2TiI_6/PCBM/Al-based PSC photovoltaic model. The PSC material, Cs_2TiI_6 thickness, device temperature, and optical visibility were studied under optimal conditions for both the *n*-i-*p* and *p*-i-*n* structured models using a 1.5G spectrum Solar Cell Capacitance Simulator – 1 Dimension simulator (SCAPS-1D). The *n*-i-*p* model (regular) showed that Cs_2TiI_6-based PSC has optimum photovoltaic performance at 500 nm thickness, where photovoltaic performance is recorded as V_{OC}: 0.76 V, J_{SC}: 13.69 mA/cm^2, PCE: 7.6 %, and FF: 76 %, and the *p*-i-*n* model (inverted) revealed that Cs_2TiI_6-based PSC has the highest PV performance at 400 nm thickness, where photovoltaic indices are recorded as V_{OC}: 0.63 V, J_{SC}: 14.22 mA/cm^2, PCE: 6.7 %, and FF: 70 %. On the other side, both *n*-i-*p*-structured FTO/TiO_2/Cs_2TiI_6/Spiro-OMeTAD/Au and *p*-i-*n*-structured FTO/PEDOT:PSS/Cs_2TiI_6/PCBM/Al-based PSC models have optimum device temperatures at 30 °C. The visible range for the *n*-i-*p* model and the *p*-i-*n* model-based device is 1000 nm and 900 nm wavelength, respectively.

Keywords: Cs_2TiI_6, Perovskite, EQE, PV, Thickness, PCE.

DOI: 10.21272/jnep.18(2).02022 PACS number: 88.40.jm

1. INTRODUCTION

PV (photovoltaic) energy is one of the cleanest energy sources in the world, and it is one of the most in-demand renewable energy resources in India [1-2]. PV technology rapidly developed from first generation to fourth generation with the discovery of new materials like the perovskite solar cell (PSC) materials due to their superior opto-electrical, mechanical, and structural properties like band gap, carrier mobility, absorption coefficient, and diffusion length [3-5]. But a few disadvantages make it not suitable for commercialization: toxic nature due to the Pb-element and device instability. Thus, the advancement of lead-free PSC materials has developed a new interest among the scientists to overcome the above-mentioned problems. In general terms, titanium (Ti) is a low-toxic planet-rich element that can be a perfect contender to substitute the Pb element from PSC. Initially, Ju *et al.* (2018) developed a cesium titanium (IV)-based halide PSC, which has a tunable band gap between 1.0 eV and 1.8 eV [6]. After that, Chen *et al.* (2018) developed an FTO/TiO_2/Cs_2TiBr_6/P_3HT/Au-based planar structure, and later they added a C_{60} layer to improve the performance of the device. They also showed that Cs_2TiBr_6-based PSC was degraded in air easily [7]. Chakraborty *et al.* (2019) showed a theoretical study of four Ti-based halide materials viz., Cs_2TiBr_6, Cs_2TiI_6, Cs_2TiCl_6, and Cs_2TiF_6, which have very low power conversion efficiency [8].

Our study focuses on the development of an n-i-p structure FTO/TiO_2/Cs_2TiI_6/Spiro-OMeTAD/Au-based PSC model and a *p*-i-*n* structure FTO/PEDOT:PSS/Cs_2TiI_6/PCBM/Al-based PSC model. Later, the optimization of PSC thickness and their PV performance was also studied to understand the device morphology and its effect on device PV performance. The effect of device temperature on both the *n*-i-*p* and *p*-i-*n*-based device structures was also analysed to find the optimum device temperature. The optical visible range of both the *n*-i-*p* and *p*-i-*n*-based PSCs is discussed through an external quantum efficiency study.

2. DEVICE STRUCTURE AND SIMULATION

The proposed device structure is of two types: a) the

* Correspondence e-mail: kunal.eiilm.vu@gmail.com
† narmadhar2014om@gmail.com

Cite this article as: K. Chakraborty et al., *J. Nano- Electron. Phys.* 18 No 2, 02022 (2026) https://doi.org/10.21272/jnep.18(2).02022

n-i-*p* model: FTO/TiO_2/Cs_2TiI_6/Spiro-OMeTAD/Au; b) the *p*-i-*n* model: FTO/PEDOT:PSS/Cs_2TiI_6/PCBM/Al. The schematic diagram of the two types of device structure is shown in Fig. 1. A Solar Cell Capacitance Simulator – 1 Dimension simulator-was incorporated to perform the entire simulation work.

Table 1 – *n*-i-*p* model various device parameters [8-12]

Parameters	FTO	Cs_2TiI_6	TiO_2	Spiro-OMeTAD
λ (nm)	150	varied	50	100
E_g (eV)	3.6	1.02	3.2	3.2
E_a(eV)	4.5	4	4.1	2.1
ζ_r	10	5.36	9	3
μ_n (cm²/vs)	100	0.236	20	2×10^4
μ_h (cm²/vs)	20	0.171	10	2×10^4
N_D (cm^{-3})	0	3×10^{19}	1×10^{19}	0
N_A (cm^{-3})	1.8×10^{19}	3×10^{18}	0	10^{20}

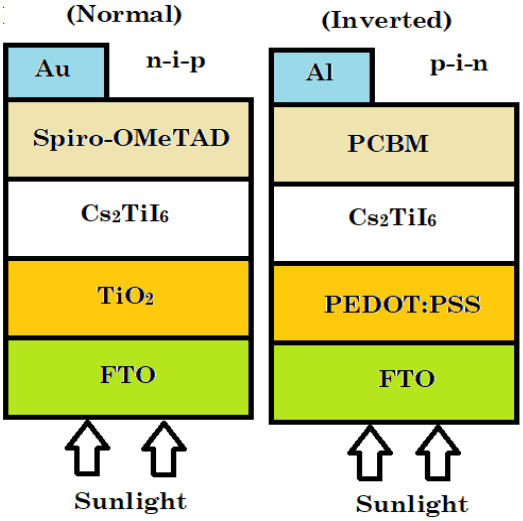

Fig. 1 – Schematic diagram of *n*-i-*p* and *p*-i-*n* model

Our study showed the effect of active layer thickness and device temperature on device PV performance. The device parameters used in that simulation process are mentioned in Table 1 for the *n*-i-*p* model and in Table 2 for the *p*-i-*n* model, and their various parameters are defined as λ: thickness, E_g: band gap, E_a: electron affinity, ζ_r: relative permittivity, N_D: donor density, N_A: acceptor density, μ_n: electron mobility, and μ_h: hole mobility, etc.

Table 2 – *p*-i-*n* model various device parameters [8-12]

Parameters	FTO	Cs_2TiI_6	PEDOT:PSS	PCBM
λ (nm)	150	varied	40	80
E_g (eV)	3.6	1.02	3	2.1
E_a(eV)	4.5	4	2.78	3.9
ζ_r	10	5.36	2.2	3.9
μ_n (cm²/vs)	100	0.236	1×10^{-5}	0.001
μ_h (cm²/vs)	20	0.171	3.2×10^{-4}	0.002
N_D (cm^{-3})	0	3×10^{19}	0	1×10^{16}
N_A (cm^{-3})	1.8×10^{19}	3×10^{18}	6×10^{16}	1×10^{19}

Various PV performance indices, including open circuit voltage (V_{OC}), short circuit current density (J_{sc}), power conversion efficiency (PCE), and fill factor (FF), were calculated for both the *n*-i-*p* and *p*-i-*n* device models using above-mentioned device parameters [13-14].

3. RESULTS AND DISCUSSION

3.1 *n*-i-*p* Model Performance Analysis

For this work, the thickness of Cs_2TiI_6-based PSC was changed from 100 to 700 nm, and their PV performance in terms of V_{OC}, J_{SC}, PCE, and FF parameters was recorded. The simulated result is plotted in terms of V_{OC}-thickness; PCE-thickness is depicted in Fig. 2. From this figure, it is clearly observed that both the V_{OC} and PCE initially rise with the thickness increase up to 500 nm significantly. The main reason behind that incident is that a much thicker absorbing layer can absorb higher photons, and as a result, the PCE of the device increases [15-16]. After that 500 nm thickness, there is no clear evidence of significant changes in the PV performance, which implies that after 500 nm thickness, the back recombination process in the device will start [17-18].

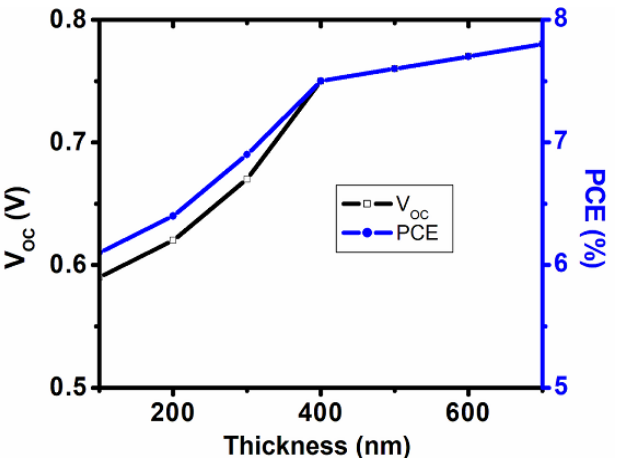

Fig. 2 – Variation of V_{OC}, PCE with the thickness of the PSC

3.2 *p*-i-*n* Model Performance Analysis

The *p*-i-*n* model is also referred to as the inverted model. To understand the PV performance along with the thickness of the absorbing layer, we have performed the simulation work by varying the thickness of the Cs_2TiI_6-based PSC layer from 100 to 700 nm. The V_{OC}-PCE changes with the thickness of the Cs_2TiI_6-based PSC are depicted in Fig. 3. Initially, both V_{OC} and PCE started to rise as the thickness started to increase from 100 nm. From the figure it is seen that till 400 nm thickness, there is a clear increment in the V_{OC} and PCE, but after 400 nm thickness, there are no significant changes in the V_{OC}, and PCE is observed. So, the optimized thickness for the inverted model is 400 nm.

3.3 Effect of Device Temperature

The effect of device temperature on device performance is depicted in Fig. 4. Here, the

temperature of the device is varied from 10 °C to 70 °C. From this figure, it is clearly visible that up to 30 °C temperature, the device PCE increases for both the *n*-i-*p* and *p*-i-*n* architecture models. After that 30 °C temperature, the PCE of the device remained almost constant. The increment in device temperature will lead to a fall in V_{OC}, and as a result, PCE also started to decrease slowly. Thus, higher temperature may also lead to recombination of charge carriers [19-20].

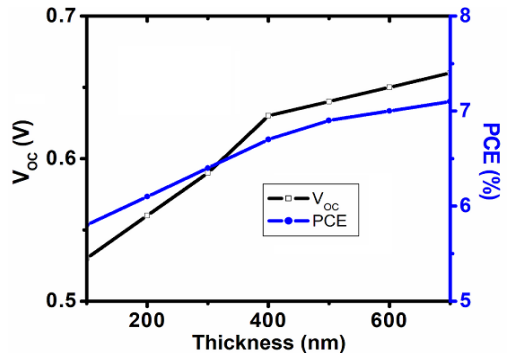

Fig. 3 – Variation of V_{OC}, PCE with the thickness of the PSC

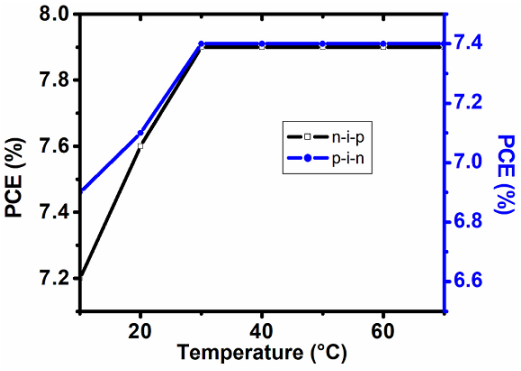

Fig. 4 – Effect of temperature on device performance

3.4 Study of External Quantum Efficiency

EQE (external quantum efficiency) is defined as the number of charges produced due to the complete incidence of photons [8, 12]. Here, Fig. 5 shows the EQE plot of the PSC where wavelength is varied from 100 to 1000 nm. From that Fig. 5, it is observed that the *n*-i-*p* model is active up to 1000 nm wavelength, whereas the *p*-i-*n* model is active up to 900 nm. Both the *n*-i-*p* and *p*-i-*n* models have optimum EQE at 600 nm wavelength. But the *n*-i-*p* model has a slightly better visible range than the *p*-i-*n* model.

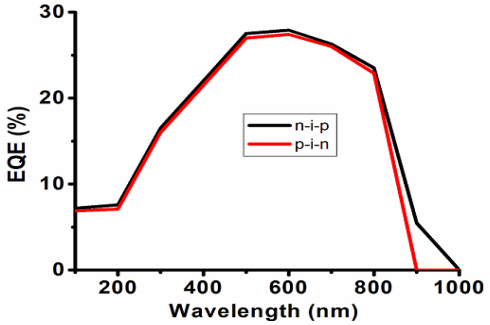

Fig. 5 – EQE plot of the *n*-i-*p* and *p*-i-*n* device model

3.5 Study of Optical Properties

Here, Fig. 6 shows the optical absorption coefficient plot of the *n*-i-*p* and *p*-i-*n* structure device. From that figure, it is clear that at 100 nm thickness both the device has optimum optical absorption coefficient (alpha) and after that thickness the optical absorption coefficient is started to fall. So, much thicker absorbing layer has low optical absorption coefficient.

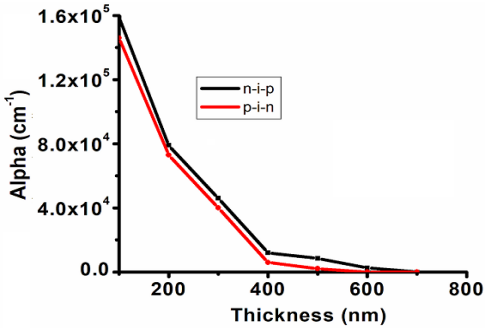

Fig. 6 – Absorption coefficient plot of the *n*-i-*p* and *p*-i-*n* device

3.6 *J-V* plot of the device

The *J-V* plot of the *n*-i-*p* and *p*-i-*n* structure device under optimized condition is depicted in Fig. 7. The optimized values of PV parameters are tabulated in Table 3 and Table 4.

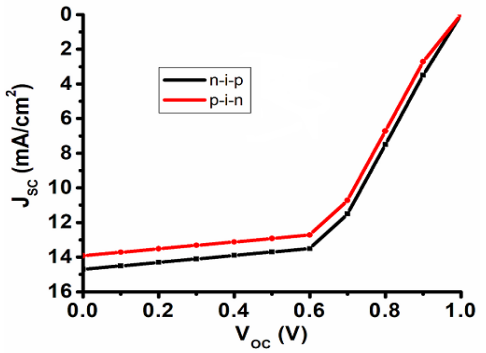

Fig. 7 – *J-V* plot of the *n*-i-*p* and *p*-i-*n* device

Table 3 – *n*-i-*p* model PV performance

Material	V_{OC} (V)	J_{SC} (mA/cm²)	PCE (%)	FF (%)
Cs_2TiI_6	0.76	13.69	7.6	76

Table 4 – *p*-i-*n* model PV performance

Material	V_{OC} (V)	J_{SC} (mA/cm²)	PCE (%)	FF (%)
Cs_2TiI_6	0.63	14.22	6.7	70

4. CONCLUSION

Our study represents the modelling of an *n*-i-*p* and *p*-i-*n* structured device model where Cs_2TiI_6-based PSC has been used as an absorbing layer. The thickness of the *n*-i-*p* and *p*-i-*n* structured device model has been optimized. The optimized thickness for the *n*-i-*p* and *p*-i-*n* structured device models is 500 nm and 400 nm, respectively, and the optimized device temperature is 30 °C. The optical visible wavelength range for the *n*-i-*p* and *p*-i-*n* structured device model is 1000 nm and

900 nm. All the analysed results suggested that the *n*-i-*p*-based model has better PV performance than the *p*-i-*n*-based model.

ACKNOWLEDGMENT

The authors are grateful to the Dept. of Electronics and Information Systems, University of Gent, Belgium, and Prof. Burgelman for providing the SCAPS software to carry out this research work.

REFERENCES

1. A. Kojima, K. Teshima, Y. Shirai, T. Miyasaka, *J. Am. Chem. Soc.* **131** No 17, 6050 (2009) https://doi.org/10.1021/ja809598r.
2. F. Giustino, H.J. Snaith, *ACS Energy Lett.* **1** No 6, 1233 (2016) https://doi.org/10.1021/acsenergylett.6b00499.
3. S.D. Stranks, G.E. Eperon, G. Grancini, C. Menelaou, M.J. Alcocer, T. Leijtens, L.M. Herz, A. Petrozza, H.J. Snaith, *Science* **342** No 6156, 341 (2013) https://doi.org/10.1126/science.1243982.
4. W.S. Yang, J.H. Noh, N.J. Jeon, Y.C. Kim, S. Ryu, J. Seo, *Science* **348** No 6240, 1234 (2015) https://doi.org/10.1126/science.aaa9272.
5. W.J. Yin, J.H. Yang, J. Kang, Y. Yan, S.H. Wei, *J. Mat. Chem. A* **3** No 17, 8926 (2015) https://doi.org/10.1039/C4TA05033A.
6. M.G. Ju, M. Chen, Y. Zhou, H.F. Garces, J. Dai, L. Ma, N.P. Padture, X.C. Zeng, *ACS Energy Lett.* **3** No 2, 297 (2018) https://doi.org/10.1021/acsenergylett.7b01167.
7. M. Chen, M.G. Ju, A.D. Carl, Y. Zong, R.L. Grimm, J. Gu, X.C. Zeng, Y. Zhou, N.P. Padture, *Joule* **23** No 3, 558 (2018) https://doi.org/10.1016/j.joule.2018.01.009.
8. K. Chakraborty, M.G. Choudhury, S. Paul, *Sol. Energy* **194** No 12, 886 (2019) https://doi.org/10.1016/j.solener.2019.11.005.
9. S.S. Urmi, et al. *Nanomaterials* **13** No 14, 2100 (2023) https://doi.org/10.3390/nano13142100.
10. A.S. Alali, et al. *Nanomaterials* **14** No 13, 1146 (2024) https://doi.org/10.3390/nano14131146.
11. N. Rai, S. Rai, P.K. Singh, P. Lohia, D.K. Dwivedi, *J. Mat. Sci: Mat. Elec.* **31**, 16269 (2020) https://doi.org/10.1007/s10854-020-04175-z.
12. K. Chakraborty, S. Paul, U. Mukherjee, S. Das, *J. Nano-Electron. Phys* **13** No 3, 03009 (2021) https://doi.org/10.21272/jnep.13(3).03009.
13. K. Chakraborty, M.G. Choudhury, S. Paul, *IEEE Trans. Dev. Mat. Reli.* **21** No 4, 465 (2021) https://doi.org/10.1109/TDMR.2021.3106340.
14. K. Tan, P. Lin, G. Wang, Y. Liu, Z. Xu, Y. Lin, *Solid-State Electron.* **126** No 12, 75 (2016) https://doi.org/10.1016/j.sse.2016.09.012.
15. K. Chakraborty, M.G. Choudhury, S. Paul, *IEEE J. Photovolt.* **11** No 2, 386 (2021) https://doi.org/10.1109/JPHOTOV.2021.3050268.
16. N. Chaudhary, R. Chaudhary, *J. Mat. Chem. C* **3** No 45, 11886 (2015) https://doi.org/10.1039/C5TC03124A.
17. Y. Yang, J. You, *Nature* **544** No 4, 155 (2017) https://doi.org/10.1038/544155a.
18. A. Zhang, Y. Chen, J. Yan, *IEEE J. Quan. Electron.* **52** No 6, (2016) https://doi.org/10.1109/JSSC.2017.2647925.
19. Shubham, Raghvendra, C. Pathak, S.K. Pandey, *IEEE Trans. Elec. Dev.* **67** No 7, 2837 (2020) https://doi.org/10.1109/TED.2020.2996570.
20. I. Matacena, L. Lancellotti, N. Lisi, P.D. Veneri, P. Guerriero, S. Daliento, *Energies* **13**, 1908 (2020) https://doi.org/10.3390/en13081908.

Аналіз продуктивності структурованого *n*-i-*p* та *p*-i-*n* перовскітного сонячного елемента без свинцю на основі Cs_2TiI_6

K. Chakraborty[1], R. Narmadha[2], Islom Kadirov[3], Visalakshi Narapareddi[4], Ranjan Kumar Mahapatra[5], Karedla Chitambara Rao[6]

[1] *Department of Electrical Engineering, IMPS College of Engineering and Technology, Malda, W.B, India*
[2] *Department of Mechatronics, Sathyabama Institute of Science and Technology, Chennai, T.N, India*
[3] *Department of Transport Systems, Urgench State University, Urgench, Uzbekistan*
[4] *School of Business, Aditya University, Surampalem, A.P, India*
[5] *Department of Electronics and Communication Engineering, Koneru Lakshmaiah Education Foundation, Guntur, A.P, India*
[6] *Department of Electronics and Communication Engineering, Aditya Institute of Technology and Management, Tekkali, A.P., India*

У цій роботі показано розробку фотоелектричної моделі PSC на основі FTO/TiO_2/Cs_2TiI_6/Spiro-OMeTAD/Au з *n*-i-*p* структурою та *p*-i-*n* структурою на основі FTO/PEDOT:PSS/Cs_2TiI_6/PCBM/Al. Матеріал PSC, товщина Cs_2TiI_6, температура пристрою та оптична видимість досліджувалися за оптимальних умов для моделей з *n*-i-*p* та *p*-i-*n* структурою за допомогою симулятора ємності сонячних елементів зі спектром 1,5 Г – 1 вимір (SCAPS-1D). Модель *n*-i-*p* (звичайна) показала, що PSC на основі Cs_2TiI_6 має оптимальну фотоелектричну продуктивність при товщині 500 нм, де фотоелектрична продуктивність зафіксована як V_{OC}: 0,76 В, J_{SC}: 13,69 мА/см^2, PCE: 7,6 % та FF: 76 %, а модель *p*-i-*n* (інвертована) показала, що PSC на основі Cs_2TiI_6 має найвищу фотоелектричну продуктивність при товщині 400 нм, де фотоелектричні індекси зафіксовані як V_{OC}: 0,63 В, J_{SC}: 14,22 мА/см^2, PCE: 6,7 % та FF: 70 %. З іншого боку, як моделі PSC на основі *n*-i-*p*-структури FTO/TiO_2/Cs_2TiI_6/Spiro-OMeTAD/Au, так і моделі PSC на основі *p*-i-*n*-структури FTO/PEDOT:PSS/Cs_2TiI_6/PCBM/Al мають оптимальну температуру пристрою на рівні 30 °C. Видимий діапазон для моделі *n*-i-*p* та пристрою на основі моделі *p*-i-*n* становить довжину хвилі 1000 нм та 900 нм відповідно.

Ключові слова: Cs_2TiI_6, Перовскіт, EQE, PV, Товщина, PCE.